Unmasking Inhibition Prolongs Neuronal Function in Retinal Degeneration Mouse Model

Qin Wang1, Seema Banerjee1, Chung Him So1, Chunting Qiu1, Hang I Christie LAM1, Dennis Tse1, Béla Völgyi3, Feng Pan1,2*

1: School of Optometry, The Hong Kong Polytechnic University, Kowloon, Hong Kong.
2: The Centre for Eye and Vision Research, Hong Kong
3: Department of Experimental Zoology and Neurobiology, Szentágothai Research Centre, MTA NAP Retinal Electrical Synapses Research Group, University of Pécs, Hungary

*Corresponding author: Feng Pan, School of Optometry, The Hong Kong Polytechnic University, Hung Hom, Hong Kong.
Tel: +852 2766 6640; Fax: +852 2764 6051; Email: feng.a.pan@polyu.edu.hk

Abbreviations:

c/d	cycle per degree
CNS	Central Nervous System
EPSCs/IPSCs	Excitatory/Inhibitory postsynaptic currents
ERGs	Electroretinograms
GABA	Gamma-aminobutyric acid
PB	Phosphate buffer
PBS	Phosphate buffered saline
pSTR/nSTR	positive/negative scotopic threshold response
PTX	Picrotoxin
RP	Retinitis Pigmentosa
RGCs	Retinal ganglion cells
S.E.M	Standard error of the mean
TPMPA	1,2,5,6-tetrahydropyridin-4-yl-methylphosphinic acid
WT	Wild-type

Abstract:

All neurodegenerative diseases involve a relatively long period of timeframe from the onset of the disease to complete loss of functions. Extending this functional timeframe as close to normal as possible would improve the quality of life of patients with neurodegeneration. The retina, as the part of central nervous system and the target of neurodegenerative disease, provides an ideal model to investigate this strategy. Retinitis Pigmentosa (RP) causes degeneration of photoreceptors and, ultimately, blindness. Although the rate of progression and degree of visual loss varies, there is usually a prolonged time before patients totally lose their photoreceptors and vision. Currently no intervention exists for long-term photoreceptor rescue. It is believed that inhibitory mechanisms are still intact and may become relatively strong after gradual loss of photoreceptors in RP patients. Therefore, it is possible that light response of remained photoreceptors and visual information processes in retinal circuits still exist and function well, but hyperactive inhibition in the inner retina masks the visual signalling process. Our results indicate that if the inhibition in the inner retina was unmasked, the retina of the rd10 mouse (the well-characterized RP mimicking, clinically relevant mouse model) can induce light responses of many retinal ganglion cells and restore their normal light sensitivity. A feedback effect mediated by GABA A receptor plays a major role in this masking inhibition. ERG b-wave and behavioural tests of spatial vision partly recovered after PTX application. Hence, results of this study show that removing retinal inhibition unmasks signalling mediated by surviving cones. Furthermore, these results may offer a potential strategy to restore the light response with the surviving cones in the rd10 mouse retinas- a possible similar approach to help patients with RP and other neurodegenerative diseases.

Introduction:

In many chronic neurodegenerative diseases, such as Parkinson's and Alzheimer's diseases of the brain; macular degeneration, retinitis pigmentosa, and glaucoma of the eye, it takes a relatively long period of time from the commencement of the degenerative process of the neuronal tissue to total loss of functions[1-3]. Exploring this "window" to restore the functions of the affected neurons to boost the quality of life for these patients is a plausible strategy. The retina, as part of the central nervous system (CNS) and the site of many neurodegenerative diseases, is an excellent tissue to evaluate this strategy, because of its ease of accessibility and the many investigative tools available [4].

Retinitis Pigmentosa (RP) is a group of diseases involving degeneration of photoreceptors with consequential blindness. It affects 1:4-5000 live births and is typically diagnosed in adolescents and young adults with the average age of diagnosis of 35.1 years[5]. Disease symptoms begin with night blindness followed by a progressive loss of peripheral vision that often ends in total blindness. The rate of progression and degree of visual loss varies from person to person[6]. Currently there is no approved treatment for this disease[7].

In humans with RP, cones tend to be preserved until most of the rods have died. Once most rods have been eliminated, the rate of cone degeneration accelerates but its extent and timeframe differ among individuals. This may be due to genetic expression differences in rods and cones, and in environmental exposures[8]. One of the best known and most commonly used animal models for studying genetically linked retinal degenerations is the rd mouse [9]. In this mouse, rod photoreceptors degenerate due to a mutation in the beta-subunit of cGMP phosphodiesterase (PDE), essential for phototransduction to produce the light response[10]. Mutations in PDE also cause RP in humans[11]. Mice homozygous for the rd10 mutation show retinal degeneration with sclerotic retinal vessels at four weeks of age. Histology at three weeks of age shows retinal degeneration[12].

The maximal response to electroretinograms (ERGs) of homozygote rd10 mice occurs at three weeks of age and is non-detectable at two months of age. Their rod outer segments never develop, and rods start degenerating in the second week after birth. This degeneration is funduscopically detectable as pigmentary retinopathy. Only about 2% of rods remain in the posterior region at postnatal day 17 and almost none by day 36. In contrast, 75% of the cone nuclei remain at day 17. These cones disappear slowly, but about 1.5% of the original population of cones are still present at 18 months of age[13]. Normally, rods will all die after postnatal day 38 (P38) and cones begin to be affected noticeably from P38-46[14]. Noticeably, there is a long "window" in time before the mouse loses almost all their photoreceptors, which is

similar to what is observed in human RP patients. However, currently there are no reports of long-term restoration of rod photoreceptor function in these animal models.

Unmasking of input signals under physiologic conditions is well documented in the brain[15], and recently it has also been reported in the retina[16]. Our previous research has indicated that inhibition controls the threshold responses of retinal ganglion cells (RGCs) under dim ambient light[17]. Dynamic modulation of this masking inhibition in the retina could serve as a mechanism for neural adaptation by altering the threshold of RGCs activities to changes in the visual environment; a strategy that may be useful to overcome the redundant information generated in the retina[17].

This study attempted to take advantage of this pre-existing physiologic masking of input signals in the RP affected retina to unmask the responses to light perception by the surviving photoreceptors. Our hypothesis is that some of the light-responding signals from the surviving photoreceptors are masked in the inner retina. This means that the synaptic currents are not translated into a spike code resulting in the lack of light response of RGCs, the output neurons of the retina. Therefore, understanding the masked inhibition and dynamic modulation of the inhibition in the retina can be a novel therapeutic strategy to restore vision in RP patients and other retinal degenerative diseases with some surviving photoreceptors.

We found that unmasking inhibition achieved by Picrotoxin (PTX) application induced a light response, implying that feedback inhibition played a major role in the inhibition. Behavioural measures of spatial vision in rd10 mouse eyes and ERG showed vision improvement with PTX application. Thus, unmasking inhibition might be translated to clinical management of neurodegenerative disease to provide a cost-effective measure and limit the impact of side effects and deterioration of quality of life.

Methods:

Animal preparation:

Rd10 mice (RRID:MGI: 3581193; B6.CXB1-Pde6b rd10 /J; Jackson laboratory Stock No: 004297), were a kind gift from Bin Lin, School of Optometry, the Hong Kong Polytechnic University. Rd10 mice are the mouse model of RP with mutations in the beta subunit of rod-specific phosphodiesterase gene 6 (PDE6β) in exon 13, which causes the massive degeneration of rod photoreceptors followed by gradual degeneration of cones. Mutations in this gene also happened in patients with autosomal recessive RP, which make the rd10 mouse a relevant model for human RP[18]. Adult (postnatal day 38–46) C57BL/C57BL:129 wild-type (WT) were used as a control group for postnatal day 38-42 (P38-46) rd 10 mice. P38-46 rd10 mice are used because all rods die after P38 and cones begin to be affected from P38-46[14]. During this stage, the cone light response is damaged [13, 19, 20]. Rd10 mice retinas were also observed after P38 when all rods had died. P41 rd10 mice were used in ERG and behavior measurements is that the results of behavior measurement were uncertain after P42. After P44 to P45 and the effects of PTX on ERG test were also inexplicit.

Animals were maintained in 12 hours–12 hours' day–night cycle. The mice were anaesthetized deeply with an intraperitoneal injection of ketamine and xylazine [80 and 10 mg/kg (body weight), respectively], and lidocaine hydrochloride (20 mg/ml) was applied locally to the eyelids and surrounding tissue.

Flattened retina preparation:

Eyes were removed under dim red illumination. For patch-clamp recordings, retinas were dissected into four equal quadrants and attached to a modified translucent Millicell filter ring (Millipore, Bedford, MA, USA). The flattened retinas were superfused with oxygenated mammalian Ringer's solution [21]. The bath solution was continuously bubbled with 95%O_2–5% CO_2 to maintain the temperature at ~32°C. Details of the procedures have been previously published [17, 22]. Anaesthetized animals were killed by cervical dislocation immediately after the enucleations.

Immunocytochemistry:

The retinal pieces were fixed in 4% paraformaldehyde for at least 10 minutes before further immunocytochemical experiments. The tissues were then incubated in the primary antibodies for 3–7 days at 4°C, followed by incubation in the secondary

antibodies overnight at 4°C. After washing with 0.1 M PB the tissues were mounted for observation.

Quantification of surviving cones stained with red/green opsins (rabbit anti-red/green opsin 1:500, Chemicon, Temecula, CA) was conducted in retinal whole-mounts[14]. For comparison purposes, all retinal samples were obtained from the dorsal section of the mid-peripheral retina in the nasotemporal plane.

To analysis of outer nuclear layer (ONL) in Figure 1-A and B, mouse retinas were fixed in 4% paraformaldehyde in 0.1 m phosphate buffer, pH 7.4, for 15 min and rinsed in 0.1 m phosphate buffer (PB), pH 7.4, to be processed for immunohistochemistry. Retinal tissues were embedded in agarose, and sections were cut 30–50 μm thick on a Vibratome (model VT1200 S; Leica Microsystems, Bannockburn, IL, USA)[23].

To measure dendritic field equivalent diameter and somata size parameters, each cell was measured from a two-dimensional projection. Maximum projection images were used for determining the area of RGCs' dendritic fields. A polygon was drawn by marking the edges of dendrites in the image with Zen 2.3 microscope software from ZEISS Microscopy. Soma area was acquired by Image J software (ImageJ, An open source developed by National Institutes of Health, Bethesda, MD, United States, 1.52i, RRID:nif-0000-30467)[24]. Subsequently, the polygon area, the equivalent diameter and the major axis were calculated. The dendritic field equivalent diameter (Figure 2E) is $2\sqrt{A/\pi}$, where A is the polygon area. To compare the stratification of RGCs in WT and rd10 mouse retinas in Figure 2, dendrites of RGCs were acquired in confocal image stacks. Subsequently, the ChAT bands were used as reference and dendritic density was calculated versus the resulting IPL depth [25].

Light Stimulation:

A green (λ=525 nm) light-emitting diode (HLMP-CM3A-Z10DD, Broadcom Limited, San Jose, CA, USA) was used to deliver uniform full-field visual stimuli to the surface of the retina. The intensity of the square wave light stimuli was calibrated and expressed in terms of the time-averaged rate of photoisomerizations per rod per second (Rh* per rod/sec)[17]. Recordings were performed in dark-adapted conditions.

Electrical recording

Extracellular recordings were obtained from single retinal ganglion cells of the mid-peripheral retina in the nasotemporal plane. Recordings were performed by using an Axopatch 700B amplifier connected to a Digidata 1550B interface and

pCLAMP 10 software (Molecular Devices). Cells were visualized with near infrared light (>775 nm) at ×40 magnification with a Nuvicon tube camera (Dage-MTI, Michigan City, IN, USA) and differential interference optics on a fixed-stage microscope (Eclipse FN1; Nikon, Tokyo, Japan). Retinas were superfused at a rate of 1−1.5 ml min−1 with Ringers solution, composed of (mM): 120 NaCl, 2.5 KCl, 25 $NaHCO_3$, 0.8 Na_2HPO_4, 0.1 NaH_2PO_4, 1 $MgCl_2$, 2 $CaCl_2$ and 5 D-glucose. The bath solution was continuously bubbled with 95% O_2–5%CO_2 at 32°C. Electrodes were pulled to 5−7 MΩ resistance, with internal solutions consisting of (mM): 120 potassium gluconate, 12 KCl, 1 $MgCl_2$, 5 EGTA, 0.5 $CaCl_2$, and 10 HEPES (pH adjusted to 7.4 with KOH). This internal solution was used in experiments, in which spiking was not blocked. In whole-cell or perforated-patch (with β-escin) recordings, to improve the space clamp and to block spiking, the internal solution contained QX-314 (0.5 mM) and caesium methanosulfonate instead of potassium gluconate. Absolute voltage values were corrected for 11 mV liquid junction potential in the caesium-based intracellular solution. The excitatory and inhibitory current responses were recorded approximately at the chloride or cation equilibrium/reversal potentials, −68 and 0 mV, respectively [17].

Spike trains were recorded digitally at a sampling rate of 10 kHz with Axoscope software, which were sorted by using an Off-line Sorter (Plexon, Dallas, TX, USA) and NeuroExplorer (Nex Technologies, Littleton, MA, USA) software.

Pharmacology reagents included PTX, strychnine, SR-95531, 1,2,5,6-tetrahydropyridin-4-yl-methylphosphinic acid (TPMPA), SCH 23390, and eticlopride obtained from Sigma-Aldrich (St Louis, MO, USA).

Intensity–response profiles for individual cells were generated by calculating spike counts in 1000 ms bits before, during and after the presentation of a stimulus of 1000 ms duration, with intensities varied over 5 log units. The number of light-evoked ON and OFF spikes of RGCs were calculated by subtraction of the background spike or current activity from those evoked by the light stimulus onset and offset, respectively. Averaged response data were then normalized and plotted against the intensity of the light stimuli using Origin software (OriginLab, Northampton, MA, USA). Data points were fitted by the classic Michaelis–Menten equation[26], as follows:

$$R = \frac{R_{max} \cdot I_a}{I_a + \alpha_a}$$

Where R is the measured response, Rmax the maximal response, I the stimulus intensity, σ the light intensity that produces a response of 0.5 Rmax, and a is the Hill coefficient. Response thresholds for individual cells were taken as 5% of the maximal spike frequency. Population histograms of response thresholds were fitted

by non-linear regression[17].

Cell identification:

The recorded cells were dye-injected with pipette tips filled with 4% Neurobiotin (Vector Laboratories, Burlingame, CA, United States) and 0.5% Lucifer Yellow-CH (Molecular Probes, Eugene, OR, United States) as routine[27]. The images of the cell were acquired on a Zeiss LSM 800 with an Airyscan (Zeiss, Thornwood, NY, United States) confocal microscope. A z-stack of images was acquired at 0.35 μm steps at a resolution of 1024 × 1024 pixels. The precise depth of RGC dendritic stratification was confirmed by immunostaining against goat anti-ChAT(1:500; Millipore; Cat# AB144P, RRID:AB_2079751) to label the ON and OFF layers in the mouse inner plexiform layer.

ERG procedure:

Prior to the test, the animals were dark adapted overnight (at least 17 h) in the experimental room. All subsequent handling and preparations were performed under dim red light. The animals were anaesthetized with a weight-based intraperitoneal injection of a solution containing Ketamine 100 mg/ml and Xylazine 20 mg/ml. The corneas of both eyes were anesthetized with Proxymetacaine 0.5% (Provain-POS, Ursapharm, Saarbrücken) and the pupils were dilated using a drop of Tropicamide 1.0% (Mydriacyl, Alcon). The animals were then placed on a warming table filled with heated water maintained at 37°C. A drop of 3% Carbomer 974P gel (Lacryvisc, Alcon) was applied to the eye to prevent corneal dehydration. A gold wire corneal electrode (inner ring diameter: 3mm; wire diameter: 0.5mm) was used as the active electrode. Two platinum needle electrodes were inserted subcutaneously at the base of the tail and the forehead as the ground and reference electrodes, respectively. Impedance of the active and reference electrodes was maintained at less than 15kΩ. After positioning the electrodes, the animals were remained in complete darkness for five minutes before the start of the experiment.

A Ganzfeld bowl (Q450, Roland Consult) was used to deliver visual stimuli with white light emitting diodes. Stimulation and data recording were performed using the RETI-Port® system (Roland Consult). The signals were amplified and band-pass filtered from 1 to 30 Hz and 0.1 to 1000Hz, respectively, for scotopic threshold response (STR) and scotopic ERG. Stimuli were delivered by the system spontaneously according to the customized protocol, with intensity varying from log -4.32 cd*s/m^2 to log 1.30 cd*s/m^2. To enhance the signal-to-noise ratio, the ERG waveform was averaged from multiple sweeps for STR and scotopic ERG. The time for completing the protocol was approximately 20 minutes.

Optokinetic measurements

The optomotor responses of mice were measured using the OptoMotry System (CerebralMechanics). The photopic vision was tested with background light of ~70 cd *s/m^2. OptoMotry software was used with the screens of contrasting bars of light not visible to the investigator and the investigator was blinded to the groups to minimize human bias. Visual acuity testing was performed at 100% contrast with varying spatial frequency thresholds, while contrast sensitivity testing was performed at a fixed spatial frequency threshold (0.092 cycle per degree, c/d). The temporal frequency was set at 1.5 Hz for both tests. After a series of test episodes, the same computer program to determine the acuity or contrast sensitivity was applied to both eyes.

Pharmacological application of PTX

PTX (Sigma-Aldrich) was delivered to C57BL/6 mice via subcutaneous osmotic minipumps (model 2004; Alzet) in ERG and Optokinetic measurement experiments [28]. To implant the minipumps, mice were anesthetized under surgical isoflurane anaesthesia and placed on a heating pad. The minipumps were filled with PTX solution (Phosphate-buffered saline was loaded as vehicle control) and inserted subcutaneously on the dorsum by an incision 1.5 times the diameter of the pump, and the wounds closed with suture (nylon 6-0). It was found that PTX at doses of 1mM (0.015 mg/kg/d, compared to the LD50 of 3 mg/kg) had effectively induced ERG and behavior responses of rd10 mice compared to control groups. As to the electrical recording, 100μM PTX will be applied in the Ringer solution.

Data Acquisition and Analysis

Retinal whole mounts and vertical sections were acquired on a Zeiss LSM 800 with an Airyscan (Zeiss, Thornwood, NY, United States) confocal microscope using a 40× oil immersion objective (N.A. 1.3)/ 20x objective (N.A. 0.8). The retinas from the mice were imaged under identical acquisition conditions, including laser intensity, pinhole, photomultiplier amplification, and z-stack step size. Z-axis steps were usually 0.35 μm. Four fields were examined for each mouse retina, and the images processed and cell number (Figure 1 A and B) were analysed by using ImageJ software.

Statistical analyses were performed by using Origin software (OriginLab, Northampton, MA, USA). Statistical significance ($P < 0.05$) was determined by using Student's t test. The result shown are mean values ± standard error of the mean (S.E.M), unless the otherwise indicated. Polynomial fitting was applied to Figure 8 C

to F by using Origin software.

Results:

rd10 mice experiencing retinal degeneration still had surviving cones on P46.

As a model of autosomal recessive Retinitis Pigmentosa (RP), retinal degeneration 10 (rd10) mice carry a spontaneous mutation of the rod-phosphodiesterase (PDE) gene, leading to a rod degeneration that starts around P18. Later on, from P38 cones are progressively affected as well. This leaves open a time window for light responses recording from RGCs between P38 to P46 [13], when rd10 mice lost all rods and cones began to degenerate. Stained with nuclear dye DAPI, retinas of WT mice (P46) displayed 12-15 layers of photoreceptor somata in the outer nuclei layers (ONL) (12.9± 0.4, mean ± S.E.M, n=12), whereas only 1-2 layers of outer nuclei could be observed (**Figure 1 A and B**) in P46 rd10 mouse retinas (1.3± 0.2, mean ± S.E.M, n=12, p<0.01). We also utilized red/green opsin specific antisera to stain outer/inner segments and observed numerous dead cones in the P46 rd10 mouse retina s (**Figure-1 C and D**). Compared to the cone of WT mice retinas (12969± 307, mean ± S.E.M, n=8), there were significant decreases in the number of cones in the P46 rd10 mouse retina (6830± 268, mean ± S.E.M, n=8, p<0.01). However, even a week after cones start degenerating, more than half of the cones are retained and appear healthy in the P46 rd10 mouse retina.

RGCs maintain normal morphology in the P46 rd10 mouse as in WT mouse retinas

In the mouse retina, more than 40 subtypes of RGCs have been described[29-31]. This study focused on easily identified alpha-like RGCs(confirmed by cell dye labelling after recording) for the initial testing of the hypothesis [17, 22]. It had been shown previously that normal soma/dendritic structure of RGCS, and their projections to higher visual centre are retained for up to 9 months after the death of photoreceptors [32, 33]. In this study, ON alpha, OFF alpha RGC, and ON-OFF RGC were examined in both up to P46 rd10 mouse retina and in their WT counterparts. All these three types RGCs are stratified on the same IPL layer in both rd10 and WT retinas. ON alpha RGCs had spherical somata and similar somata size in both rd10 and WT retinas as well (17.9 ± 0.9μm in rd10, mean ± S.E.M, n=5; 17 ± 0.6 μm in WT, n= 18; p>0.05); Somata sizes are also similar in OFF alpha RGCs (17.3 ± 0.8 μm in rd10, n=6; 17.4 ± 0.3 μm in WT, n= 19; p>0.05) and ON-OFF RGCs (15.5 ± 0.8 μm in rd10, n=4; 16.4 ± 0.6 μm in WT, n= 6; p>0.05). As to the dendritic field equivalent diameter, there are no significant difference between rd10 and WT retinas of these 3 subtypes of RGCs: ON alpha RGCs (207± 23.4 μm in rd10, n=5; 211.1 ± 6.9 μm in WT, n= 18; p>0.05); OFF alpha RGCs (176.3 ± 7.1 μm in rd10, n=6; 193.9

± 7.2 μm in WT, n= 19; p>0.05); ON-OFF RGCs (179 ± 7.3 μm in rd10, n=4; 180.2 ± 12.7 μm in WT, n= 6; p>0.05). All three major RGC subtypes displayed very similar morphologies in the rd10 retina with those of the WT counterparts after Neurobiotin injection (**Figure 2 A to D**).

RGCs retain light-evoked EPSCs/IPSCs in the P46 rd10 mouse

Although a previous study has demonstrated that some light-evoked RGC activity can be observed till P60[34], there was no light response of most alpha-like ganglion cells in the P46 rd10 mouse retina even when light stimulation was applied in the photopic range (525 nm full field light stimulus from 0 to 108.53 Rh*/rod/s, light stimulation time: 1s). However, as shown above quite a number of cones survived up to P46 rd10 mice, and the downstream circuit and pathway appeared to be intact and functioning: as both ON-OFF RGCs and OFF alpha RGC showed light evoked response. Then, inhibitory and excitatory currents from RGCS in P46 rd10 and WT mice retinas were measured in voltage-clamped potential (-68 mV for EPSC recording and 0 mV for IPSC recordings) in response to 1 second 525nm light stimuli (light intensity= 108.53 Rh*/rod/sec).

ON alpha RGCs of both p38-46 rd10 (4 of 20 cells) and WT mouse (4 of 10 cells) were tested light evoked response to 1 second 525nm light stimuli (light intensity= 108.53 Rh*/rod/sec). Application 100μM PTX, decreased Inhibitory currents (IPSC, from 180.3 ± 9.2 to 123 ± 4.7pA, p<0.05 in rd10; from 77.3 ± 6.4 to 39 ± 4 p<0.05 in WT) but increased excitatory currents (EPSC, from 114 ± 7.1 to 221.7 ± 24.3 pA, p<0.05 in rd10; from 113. 7 ± 5.2 to 376.7 ±   16.5 pA, p<0.05 in WT) evoked by light in both mice retinas (**Figure 3A**). There is no statistically significant difference between rd10 and WT after PTX application on EPSC and IPSC (p>0.05, **Figure 3D**).

Application PTX also decreased IPSC evoked by light on OFF alpha RGCs in both rd10 (from 71 ± 4.4 to 20 ± 5.5 pA, p<0.05) and WT mouse (from 159 ± 3.5 to 109 ± 2.1 pA, p<0.05) (**Figure 3B**). PTX increased EPSC of OFF alpha RGC on both rd10 (from 159 ± 3.5 to 438.7 ± 35.5 pA, p<0.05) and WT mouse (from 71 ± 1.5 to 123.7 ± 4.6 pA, p<0.05). 4 of 18 OFF alpha RGCs were recorded in rd10 mice; 4 of 12 OFF alpha RGCs were recorded in WT mice. There is also no statistic difference between rd10 and WT after PTX application (p>0.05, **Figure 3D**).

Application PTX can decrease inhibitory currents of ON (from 252 ± 8 to 193.8 ± 5.9 pA, p<0.05) and OFF (from 266 ± 4.1 to 150.8 ± 5.3 pA, p<0.05) response but increase excitatory current of OFF response (from 614.5 ± 46.2 to 1234.3 ± 14.2 pA, p<0.05) but no ON response (from 74.8 ± 7 to 64.6 ± 4.4 pA, p>0.05) in WT retina (**Figure 3C**). PTX application only decrease IPSC of ON response in rd 10 retina

(from 300 ± 4.9 to 280 ± 2.6 pA, p<0.05) not EPSC in ON and both ON (from 247.1 ± 5.5 to 265.3 ± 1.5 pA, p>0.05) and OFF (from 52.3 ± 7 to 48 ± 1.7 pA, p>0.05) of IPSC in rd10. 4 of 16 ON-OFF alpha RGCs were recorded in rd10 mice; 6 of 9 OFF alpha RGCs were recorded in WT mice. There is also no statistic difference of ON and OFF cell responses between rd10 and WT after PTX application (p>0.05, **Figure 3D**). Normalized changed of Inhibitory currents and excitatory currents after PTX application between rd10 and WT showed that RGCs have similar cell responses in P46 rd10 and WT mouse retina.

Contrary to the fact of losing light evoked spike responses in P46 rd10 RGCs, this series of experiments demonstrated that subthreshold EPSCs were still retained and response to light stimuli. These results thus indicate that the retinal vertical signaling is functional and capable of eliciting RGCs excitatory synaptic currents, however excitatory synaptic currents were not efficiently translated into a spike response, which is possibly inhibited.

Unmasked inhibition by PTX application increased light responses in the P46 rd 10 mouse retina

It has been shown previously that GABAergic signalling masks excitatory RGC currents to fine tune light sensitivity even in the healthy mouse retina. Moreover, unmasking of these currents can be achieved by applying the relatively non-specific GABA antagonist PTX [17]. Based on our patch-clamp measurements, it can be postulated in the RP mimicking rd10 mice the inhibitory GABAergic circuit of the inner retina remains at least partially functional. The remaining cones, beginning apoptosis at P38, are capable of delivering light evoked response with the functionality of circuits. It is also hypothesized that an imbalance between excitatory and inhibitory inputs of RGCs favoured the masking inhibition. This dominant masking inhibition then prevents RGCs to translate the incoming excitatory signals into a spike code.

To test this idea, P46 retinas were tested by applying the non-specific GABAR receptor blocker Picrotoxin (PTX) to observe if the light evoked response could be restored.

Segregation of mouse RGCs based on light threshold sensitivity can be divided into four groups: high, intermediate, low-intermediate, and low sensitivity up to 4 log units' light intensities [17, 35]. After P38, only cones remain in the rd10 mouse retina, therefore, low sensitivity RGCs were expected to be recorded.

Previously the spontaneous hyperactivity of RGC in rd10 mouse retina have been observed and the intrinsic bipolar cell oscillations were shown to be responsible [19, 20, 36]. In this study, "silent" RGCs (quiescent RGCs defined by Dr.

Sagdullaev before [20]) that only produced spontaneous spikes occasionally were observed. Such RGCs, many showed OFF alpha RGC like morphology, can be suspected maintaining exacerbated masking inhibitory signals in the rd10 mouse retina. To test the idea, spiking activity from these alpha-like RGCs (n=41) were first recorded with increasing light intensities as controls (**Figure 4 A-C**). There was no light response until the stimulus intensity reached high photopic values (more than 108.53 Rh*/rod/s).

Next, 100 µM non-selective GABA receptor blocker PTX was applied for 5 min before the second set of recording started and then the same sequential light stimuli were presented (**Figure 4 D-I**). PTX application induced light response in 47.5 % of the tested "silent" RGCs. For the representative cell in Figure 4, PTX improved the threshold sensitivity to approximately 16 Rh*/rod/s stimuli (**Figure 4 D-N**). PTX application increased the light response of other RGCs in the examined population as well. The light thresholds were calculated for these examined RGCs as 18.4 ± 1.85 log units (mean ± SEM; n=19 of 40) in average, which value is similar to the low light sensitive RGC in WT retinas (**Figure 4 O**). As negative control, P56 rd01 retinas were tested with light stimuli and 100µM PTX application, no light response can be observed (**Figure 4 P-S**).

The unmasked light response is subserved mainly by GABA A receptors in rd10 mouse retina

In this experiment, the mechanism and location of masking inhibition in the inner retina was further investigated. Given that non-specific GABA blocker PTX blocks both GABA A and GABA C receptors, specific antagonists were also used to determine the contribution of each receptor in modulating GC light response in rd10 mice. Two major types of inhibition exist in the inner retina that directly or indirectly shape RGCs responses: (1) feedforward inhibition -Amacrine cells(ACs) synapse directly onto dendrites of RGCs, and (2) feedback inhibition-ACs synapse onto the axon terminals of BCs or dendrites of other ACs [37]. In the mouse retina, GABA C receptors are found exclusively presynaptic to RGCs and thereby mediate feedback inhibition [17], whereas GABA A receptors are found on AC and RGC dendrites and BC axon terminals therefore they subserve both feedback and feedforward inhibition [38]. We aimed to determine whether inhibitory circuits facilitated by ACs selectively mask inputs of the remaining cones' signals in the rd10 mouse. This also narrows down the mechanism of unmasking inhibition thus specifying further potential therapeutic target cell type.

GABA A and GABA C receptors selective antagonists, SR-95531 and TPMPA respectively, were tested in sequence to investigate the masking effect of light

response in the P40-46 rd10 mice with rod degeneration and some level of cone damage.

GABA C receptor blocker TPMPA (100 µM) was applied first, but no light response was induced (normalized responses: 0.14± 0.05; mean ± SEM, n=7)(**Figure 5 A, B and E, F; M and N**). However, light response could be induced (normalized responses: 0.86 ± 0.05; n=7) after subsequent exposure to the GABA A receptor antagonist-- SR-95531 (SR, 10µM, **Figure 5 I; J and M**). Application of SR had significant effect on light-induced response (p<0.01) **(Figure 5N)**.

In a second cohort of experiments, SR-95531 (SR, 10µM)- GABA A receptor antagonist was applied first, resulting in induction of light evoked response (normalized responses: 1.09± 0.09; n=8) (**Figure 5 C, D and G, H;M).** A following addition of GABAC receptor blocker- TPMPA (100µM) resulted no further change of the light response (normalized responses: -0.09± 0.09; n=8) (**Figure K; L and M**). Application of TPMPA had no significant effect (P =0.36) on the light induced response **(Figure 5N**). Thus, the GABA A receptor mediated exacerbated inhibition, including both feedforward and feedback inhibition, seems to play a major role in the masking RGC light responses. Similar as before, P56 rd01 retinas (n=4) were tested with light stimuli as negative control and 100µM PTX application afterward, no light response can be induced (data not shown).

Glycine receptor mediated inhibition does not contribute to the masking of RGC light responses in the rd10 mouse retina.

PTX has been shown to block glycine receptors in retinal neurons [39], suggesting that at least part of the effects of PTX on light response of RGCs could reflect a blockade of glycinergic inhibition. RGCs receiving glycinergic inputs both directly [40] and indirectly via the AII ACs/OFF cone bipolar cell signalling route that have been shown to contribute to the threshold of dark-adapted OFF RGCs [41]. To test for a potential glycinergic contribution to RGC light response masking in the rd10 mouse, the effect of glycine receptor antagonist strychnine (1 µM) was tested (**Figure 6 A to D**). Application of strychnine increased the spontaneous spike activity of α-like RGCs (n=9), but, consistent with previous studies [17] , strychnine (1µM) application did not induce the light response of silent RGCs or the increment of the S/N for the examined cells.

Unmasked RGC light responses are independent of dopaminergic circuitry

PTX has also been shown to block dopamine receptors [42]. Dopaminergic circuits affect the light sensitivity of neurons in both the inner and outer retina [42, 43]. The RGC light response induced by PTX could involve an increase in dopamine release, owing to removal of a presumed tonic inhibition and the subsequent

activation of dopaminergic circuits. To test this proposition, it was examined whether the effects of PTX on RGC light response could also be changed by blockade of dopamine receptors.

In initial experiments, application of the selective D1 receptor blocker antagonist SCH 23390 (5 µM) alone did not induce light response of RGC. However, subsequential addition of 100 µM PTX generated the light response in α like RGCs of rd10 mouse retina (7 of 22) (**Figure 7 A to F)**. The spikes of RGC recorded only increased after PTX application (**Figure 7M)**.

Similarly, sole application of the selective D2 receptor blocker eticlopride (25 µM) did not induce light response of RGC, while addition of PTX generated the light response (5 of 19) (**Figure 7 G to L)**.

Thus, the light induced responses of RGCs produced by PTX application was independent of the dopaminergic circuit. This ruled out the possibility of increased dopamine release from dopaminergic amacrine cells after their GABAergic receptors' inhibition.

GABA receptor blockade elevates the ERG b-wave not a-wave amplitudes in the rd10 mouse retina.

In vivo ERG recordings were performed in anesthetized mice to determine whether the unmasking effect due to blockade of GABA inhibition in the rd10 retina was of dominantly outer or inner retinal origin. PTX was delivered to rd10 mice via subcutaneous osmotic minipumps (model 2004; Alzet), implanted on P40 and ERG tested after 24 hours-on P41.

The positive/negative scotopic threshold response (pSTR/nSTR) showed the function of RGCs in the different time latency. Normally, pSTR appears at around 100-120ms, whereas nSTR occurs between 150 to 250ms post stimulus. In the rd10 mouse retina, the ERG response was noisy, and no typical pSTR/nSTR could be observed in control conditions. After 0.015 mg/kg/d PTX application, however, pSTR appeared around 100ms (n=6) (**Figure 8 A)**. PBS was used as vehicle control.

Compared with wild-type mice of the same age, P41 rd10 mice had lower b-wave amplitudes in the scotopic range ($P < 0.05$, n=6). Application of PTX significantly increased amplitude of b-wave ($P<0.05$) in rd10 mouse retina (**Figure 8 B, C and D**, **D** is an enlarged image of **C**). However, PTX application had no effect ($P>0.05$) on the amplitude of ERG a-wave at almost all intensities (except at 0.3 cd*s/m^2, $p<0.05$) (**Figure 8 E and F**, F is an enlarged image of **E**). In the contrast, wild-type mice of the same age had higher b-wave amplitudes in the scotopic range above -2 cd*s/m^2 ($P < 0.05$, n=6). Therefore, PTX application

induced a positive/negative scotopic threshold response and increased amplitude of ERG b-wave but not a-wave amplitude in the rd10 mouse retina.

GABA receptor blockade improves the performance of rd10 mice in behavioural tests for spatial vision

Dysfunction exemplified by a decrease in contrast sensitivity, is a clinical hallmark of RP. Behavioural model testing allows a demonstration of the lack of ability of to perceive contrast in rd10 mouse. Therefore, detecting alterations of temporal patterns in RP animal models may provide the logical basis for the PTX unmasking effect. The hypothesis in the study is unmasking via a blockade of GABA signalling could restore RGCs' light responses. Therefore, this idea will be further tested by using the optomotor response system for behavioural testing.

At the beginning of a test, the walls of the chamber appeared grey [44, 45]. The visual acuity threshold was determined with contrast set at 100%. A series of gratings of increasingly higher spatial frequencies were presented. When the mouse ceased to respond to a spatial frequency, a lower frequency grating was presented. The acuity threshold was set at the highest spatial frequency to which the animal regularly responded.

After a visual acuity threshold had been determined, a contrast threshold was tested for a series of spatial frequencies (0.031, 0.064, 0.092, 0.103, 0.192, 0.272 c/d). The initial contrast was set at 100% for each of the above spatial frequencies. The lowest contrast which elicited a response was determined and a contrast-sensitivity function calculated. Rotation of visible stimuli elicited tracking behaviour from the mouse[46]. 10 WT mice served for control measurements. To ascertain the effect of PTX, 0.015 mg/kg/d was administrated via a minipump for 48 hours. Following PTX application, mice performed the series of behavioural tests as described above. 5 of P41 rd10 mice loaded with PBS were used as vehicle control. The same experimental protocol was performed in rd10 mice as well, photopic optomotor responses of P41 rd10 mice significantly improved after PTX application ($p < 0.05$) for both the visual acuity tested at 100% contrast (increased from 0.21±0.02 to 0.29±0.016, mean ± SEM, n=6) and contrast sensitivity (tested at 0.092 cycle/degree) (decreased from 62.3 ± 6.6% to 32.6 ± 3.8%, n=6) under 1.5-Hz temporal frequency (**Figure 9)**. These behavioural tests demonstrated that the unmasking of RGC light responses via the blockade of exacerbated GABAergic inhibition in fact improved the visual acuity and the contrast sensitivity of rd10 mice.

Discussion:

Proper balance between neural excitation and inhibition is crucial to physiological functions such as in cognition and behaviour[47]. A brain dominated by excitation will result in repeated bursts of activity, similar to an epileptic seizure[48]. Conversely, a brain dominated by inhibition will silence activity, with no information being detected[49]. Similar to the brain, retinal activity functions well when a balance between excitation and inhibition generates complex patterns of activity. Inhibitory neurons are thought to shape the way excitatory neurons integrate information through synaptic interactions [50]. Thus, a seemingly simple nervous system formed with only glutamate-excitation and GABA-inhibition nonetheless results in highly complex activity [51].

Inhibition is common in the CNS, where synaptic inputs can be masked or modulated under normal physiological function[52]. Following deafferentation, such as by cutting all dorsal roots in the spinal cord, some cells show responsiveness to receptive fields outside the deafferented region that were not previously part of the responsive cells. These results suggest that deafferentation results in the unmasking of normally ineffective connections [53]. This unmasking phenomenon also exists in other CNS areas, such as the motor cortex [54]. In the CNS, some synaptic inputs under certain stimulus conditions may be masked when there are dominant inputs. These synaptic inputs are unmasked when the dominant input is removed. This unmasking may reflect an alteration in the balance of excitatory and inhibitory signalling [15].

The masked inputs may provide a possible plasticity of synaptic contacts, whereby rapid reorganization of input signalling can occur after injury[55]. In addition, unmasking of inputs reflects the normal dynamics of signalling in the brain, through which changes can be made in receptive field structure continuously as stimulus conditions vary[56]. Finally, masked inputs may come from the normal circuitry in which overlapping neuronal circuits are created during development [57]. When certain inputs repeat and dominate, the signal is "turned off" with experience to become masked.

Unmasking of input signals under physiologic conditions is well documented in the brain, and has also been reported recently in the retina [16]. The previous research indicated that inhibition controls the threshold responses of retinal ganglion cells (RGCs) under dim ambient light [17] and response delay[58]. Dynamic modulation of the masking inhibition in the retina can be a novel mechanism for neural adaptation by altering the threshold of RGCs with changes in the visual environment. For example, unmasking signals carried by the third rod pathway would be prudent at dusk or dawn, because it would increase the afferent streams carrying

visual information centrally. Modulation of the masking inhibition may occur in both dim and bright ambient light conditions. This is a useful strategy to overcome the redundant information generated in the retina. Masked excitatory signals have been found between ON and OFF visual pathways in the mouse retina [16]. Similarly, inhibitory circuitry provides a switch, which allows RGCs to change polarity rapidly from OFF to ON in the salamander [59].

In this study, GABAergic circuitry was shown to be responsible for masking the light response of alpha ganglion cells by using patch recording in rd10 mouse retinas. Application of GABA A receptor antagonist-SR had significant effect on light-induced response in p46 rd10 retina. This masking inhibition effect was mainly attributable to activation through GABA A receptors located on AC and RGC dendrites and BC axon terminals; could be feedback or feedforward or even both in in the inner retina of rd10 retina. This is contrast to our previous research, feedback inhibition via GABA C receptor contribute main role in in modulating certain RGCs light sensitivity in WT mouse[17]. Lateral inhibition in the inner plexiform layer can come from feedback (presynaptic inhibition of bipolar cell terminals) and feedforward inhibitions (postsynaptic inhibition of RGCs), which differ in RGCs involved. Feedback onto bipolar cell terminals produces a common signal that affects the function of majority RGCs postsynaptic to those terminals because there are about 10 cone bipolar cell types[60] and about more than 30 RGC types[31]. Presynaptic feedforward inhibition may only effect on less RGCs with the assumption that the amacrine cell makes exclusive contacts with these specific RGCs. Therefore, the masking inhibition effect in rd10 mouse retina included both feedforward and feedback inhibitions in unmasking light response. This might indicate more RGCs involved than WT retina to induced the light response after unmasking inhibition in rd10 retinas.

Unmasking inhibition via dopaminergic or glycinergic circuit could not restore the light response of RGCs. In contrast, unmasking inhibition via PTX application can readily restore the light response of RGCs as well visual acuity, that lead to improved performance of rd10 mice in behavioural tests of spatial vision.

The intent and design of this research was to understand the physiologic masking inhibition processes in the healthy retina and to utilize this knowledge to intervene with the goal of restoring visual signalling mediated by the surviving photoreceptors. The rd10 mouse model is a well-characterized RP mimicking, clinically relevant model. Several mutations in the same gene are known to cause RP in humans. This is clinically relevant as the fovea in the human retina consists mainly of cones and most RP patients have a remnant of cones[61]. Therefore, these studies have clinical relevance as the model is linked to human RP.

Both the methods and techniques used in this study; the knowledge about the mechanism(s) of retinal masked inhibition and its application to fight the disease may also be applicable to other neurodegenerative diseases of the retina as well as of those of the brain or other neurons. Compared with gene therapy and transplantation, pharmacologic intervention to modulate the masked inhibition in the retina is less invasive, and more economical. Therefore, future studies might provide information about whether unmasking inhibition could offer a new approach to treat other retinal degenerative disorders, and possibly diseases affecting other parts of the central nervous system.

Polls have revealed that blindness and cancer are amongst the most feared diseases[62]. The most common cause of neurodegenerative blindness is RP, for which there is currently no approved therapy available[63]. This research aimed to develop a therapeutic strategy for treatment of Retinitis Pigmentosa and to improve the quality of life of these patients. The mechanism developed in this study may also be relevant for therapies of other neurodegenerative conditions, such as Parkinson's and Alzheimer's diseases, and eye diseases including age-related macular degeneration and glaucoma that are common causes of blindness.

Limitations of the Study

The strategy of unmasking inhibition used as a treatment for diseases like neurodegeneration diseases such as RP or AMD might have a long way to achieve.

As to the spikes induced after PTX application, we did not test whether the spikes can code the effective information and then deliver the visual information to central nerve system. However, the ERG and behavior measurement might indicate this possibility.

The strategy of unmasking inhibition applied in neurodegeneration diseases had its limitation. Light-induced response can be unmasked by PTX in a "window" time - from P39 to P46 of rd10 mouse Retina. During this "window" time, there are an adequate amount of cones survived to induce light response in the degeneration status of rd10 retina. After P46, it is hard to induce light responses after 100 μm PTX application. "Window" of the strategy depended on the survival of a certain amount of cones in rd10 mouse and RP patients. Cones degeneration in the retina of RP are persistent and progressive. Its progression can differ greatly from patient to patient. However, there is a relatively long time (years) in RP patients before lost all of the cones. Thus, the "window" for strategy of unmasking inhibition will also vary among RP patients if applied.

References:

1. Gao, H.M. and J.S. Hong, *Why neurodegenerative diseases are progressive: uncontrolled inflammation drives disease progression.* Trends Immunol, 2008. **29**(8): p. 357-65.

2. Berson, E.L., *Long-term visual prognoses in patients with retinitis pigmentosa: the Ludwig von Sallmann lecture.* Exp Eye Res, 2007. **85**(1): p. 7-14.

3. Veleri, S., et al., *Biology and therapy of inherited retinal degenerative disease: insights from mouse models.* Dis Model Mech, 2015. **8**(2): p. 109-29.

4. Dowling, J.E., *The retina : an approachable part of the brain.* 2012, Cambridge, Massachusetts; London: The Belknap Press of Harvard University Press.

5. Ferrari, S., et al., *Retinitis pigmentosa: genes and disease mechanisms.* Curr Genomics, 2011. **12**(4): p. 238-49.

6. Hartong, D.T., E.L. Berson, and T.P. Dryja, *Retinitis pigmentosa.* Lancet, 2006. **368**(9549): p. 1795-809.

7. Fahim, A., *Retinitis pigmentosa: recent advances and future directions in diagnosis and management.* Curr Opin Pediatr, 2018. **30**(6): p. 725-733.

8. Campochiaro, P.A. and T.A. Mir, *The mechanism of cone cell death in Retinitis Pigmentosa.* Prog Retin Eye Res, 2018. **62**: p. 24-37.

9. Farber, D.B. and R.N. Lolley, *Cyclic guanosine monophosphate: elevation in degenerating photoreceptor cells of the C3H mouse retina.* Science, 1974. **186**(4162): p. 449-51.

10. Bowes, C., et al., *Retinal degeneration in the rd mouse is caused by a defect in the beta subunit of rod cGMP-phosphodiesterase.* Nature, 1990. **347**(6294): p. 677-80.

11. Dvir, L., et al., *Autosomal-recessive early-onset retinitis pigmentosa caused by a mutation in PDE6G, the gene encoding the gamma subunit of rod cGMP phosphodiesterase.* Am J Hum Genet, 2010. **87**(2): p. 258-64.

12. Chang, B., et al., *Two mouse retinal degenerations caused by missense mutations in the beta-subunit of rod cGMP phosphodiesterase gene.* Vision Res, 2007. **47**(5): p. 624-33.

13. Gargini, C., et al., *Retinal organization in the retinal degeneration 10 (rd10) mutant mouse: a morphological and ERG study.* J Comp Neurol, 2007. **500**(2): p. 222-38.

14. Wang, K., et al., *Retinal structure and function preservation by polysaccharides of wolfberry in a mouse model of retinal degeneration.* Sci Rep, 2014. **4**: p. 7601.

15. Barron, H.C., et al., *Unmasking Latent Inhibitory Connections in Human Cortex to Reveal Dormant Cortical Memories.* Neuron, 2016. **90**(1): p. 191-203.

16. Farajian, R., et al., *Masked excitatory crosstalk between the ON and OFF visual pathways in the mammalian retina.* J Physiol, 2011. **589**(Pt 18): p. 4473-89.

17. Pan, F., et al., *Inhibitory masking controls the threshold sensitivity of retinal ganglion cells.* J Physiol, 2016. **594**(22): p. 6679-6699.

18. Chang, B., et al., *Retinal degeneration mutants in the mouse.* Vision Res, 2002. **42**(4):
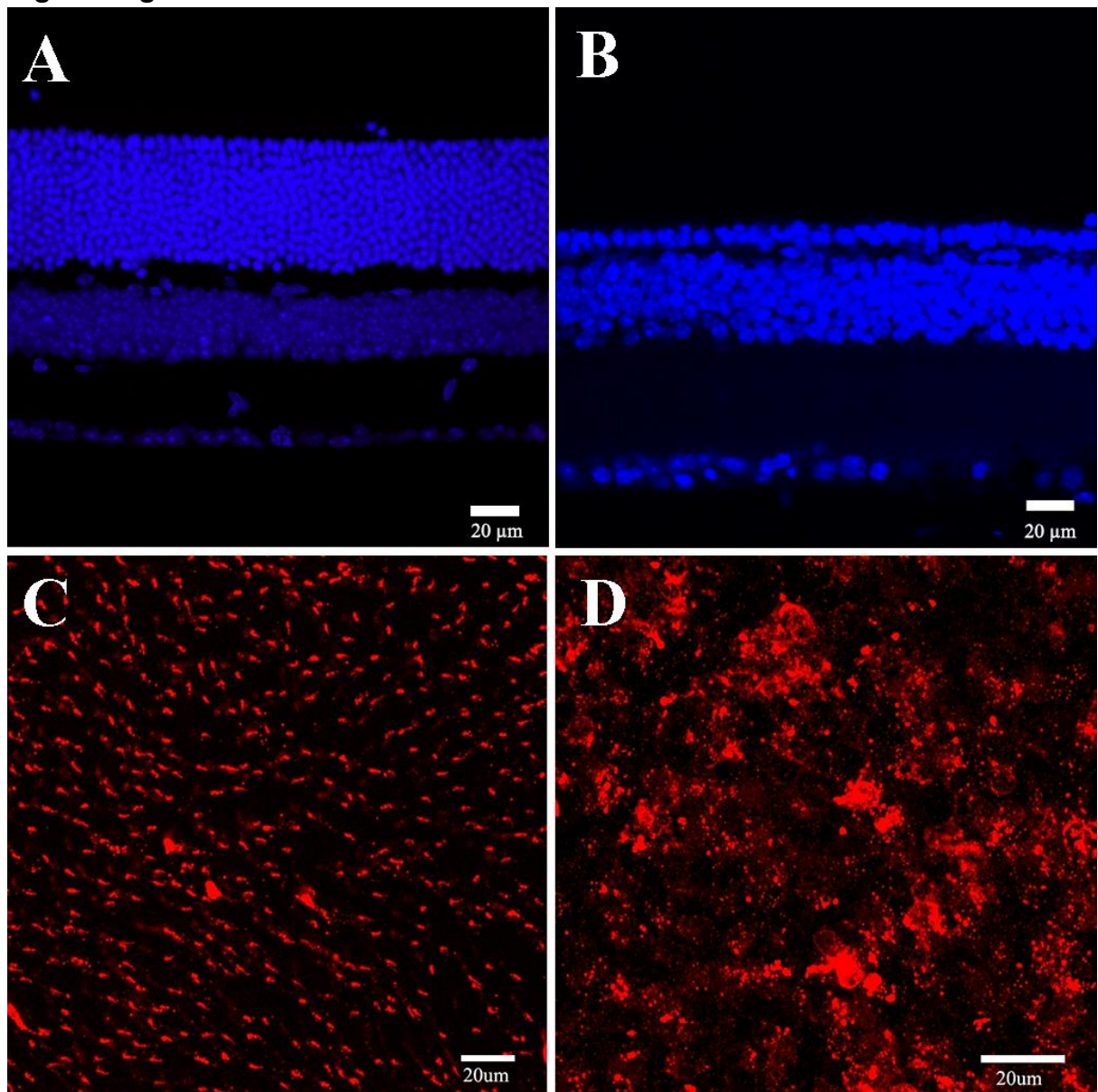
p. 517-25.

19. Stasheff, S.F., M. Shankar, and M.P. Andrews, *Developmental time course distinguishes changes in spontaneous and light-evoked retinal ganglion cell activity in rd1 and rd10 mice.* J Neurophysiol, 2011. **105**(6): p. 3002-9.

20. Toychiev, A.H., et al., *Block of gap junctions eliminates aberrant activity and restores light responses during retinal degeneration.* J Neurosci, 2013. **33**(35): p. 13972-7.

21. Bloomfield, S.A. and R.F. Miller, *A physiological and morphological study of the horizontal cell types of the rabbit retina.* J Comp Neurol, 1982. **208**(3): p. 288-303.

22. Volgyi, B., et al., *Gap junctions are essential for generating the correlated spike activity of neighboring retinal ganglion cells.* PLoS One, 2013. **8**(7): p. e69426.

23. O'Brien, J.J., et al., *Coupling between A-type horizontal cells is mediated by connexin 50 gap junctions in the rabbit retina.* J Neurosci, 2006. **26**(45): p. 11624-36.

24. Banerjee, S., et al., *Increased Connexin36 Phosphorylation in AII Amacrine Cell Coupling of the Mouse Myopic Retina.* Front Cell Neurosci, 2020. **14**: p. 124.

25. Zhang, J., et al., *Stratification of alpha ganglion cells and ON/OFF directionally selective ganglion cells in the rabbit retina.* Vis Neurosci, 2005. **22**(4): p. 535-49.

26. Thibos, L.N. and F.S. Werblin, *The properties of surround antagonism elicited by spinning windmill patterns in the mudpuppy retina.* J Physiol, 1978. **278**: p. 101-16.

27. Pan, F. and S.C. Massey, *Rod and cone input to horizontal cells in the rabbit retina.* J Comp Neurol, 2007. **500**(5): p. 815-31.

28. Akopian, A., et al., *Targeting neuronal gap junctions in mouse retina offers neuroprotection in glaucoma.* J Clin Invest, 2017. **127**(7): p. 2647-2661.

29. Volgyi, B., S. Chheda, and S.A. Bloomfield, *Tracer coupling patterns of the ganglion cell subtypes in the mouse retina.* J Comp Neurol, 2009. **512**(5): p. 664-87.

30. Pan, F., et al., *Connexin36 is required for gap junctional coupling of most ganglion cell subtypes in the mouse retina.* J Comp Neurol, 2010. **518**(6): p. 911-27.

31. Baden, T., et al., *The functional diversity of retinal ganglion cells in the mouse.* Nature, 2016. **529**(7586): p. 345-50.

32. Mazzoni, F., E. Novelli, and E. Strettoi, *Retinal ganglion cells survive and maintain normal dendritic morphology in a mouse model of inherited photoreceptor degeneration.* J Neurosci, 2008. **28**(52): p. 14282-92.

33. Lin, B. and E.B. Peng, *Retinal ganglion cells are resistant to photoreceptor loss in retinal degeneration.* PLoS One, 2013. **8**(6): p. e68084.

34. Stauffer, P.L., et al., *Gap junction communication modulates [Ca2+]i oscillations and enzyme secretion in pancreatic acini.* J Biol Chem, 1993. **268**(26): p. 19769-75.

35. Volgyi, B., et al., *Convergence and segregation of the multiple rod pathways in mammalian retina.* J Neurosci, 2004. **24**(49): p. 11182-92.

36. Borowska, J., S. Trenholm, and G.B. Awatramani, *An intrinsic neural oscillator in the*

degenerating mouse retina. J Neurosci, 2011. **31**(13): p. 5000-12.

37. Dowling, J.E. and B.B. Boycott, *Organization of the primate retina: electron microscopy.* Proc R Soc Lond B Biol Sci, 1966. **166**(1002): p. 80-111.

38. Enz, R., et al., *Immunocytochemical localization of the GABAc receptor rho subunits in the mammalian retina.* J Neurosci, 1996. **16**(14): p. 4479-90.

39. Wang, P. and M.M. Slaughter, *Effects of GABA receptor antagonists on retinal glycine receptors and on homomeric glycine receptor alpha subunits.* J Neurophysiol, 2005. **93**(6): p. 3120-6.

40. Majumdar, S., et al., *Glycine receptors of A-type ganglion cells of the mouse retina.* Vis Neurosci, 2007. **24**(4): p. 471-87.

41. Arman, A.C. and A.P. Sampath, *Dark-adapted response threshold of OFF ganglion cells is not set by OFF bipolar cells in the mouse retina.* J Neurophysiol, 2012. **107**(10): p. 2649-59.

42. Li, L. and J.E. Dowling, *Effects of dopamine depletion on visual sensitivity of zebrafish.* J Neurosci, 2000. **20**(5): p. 1893-903.

43. Herrmann, R., et al., *Rod vision is controlled by dopamine-dependent sensitization of rod bipolar cells by GABA.* Neuron, 2011. **72**(1): p. 101-10.

44. Prusky, G.T., et al., *Rapid quantification of adult and developing mouse spatial vision using a virtual optomotor system.* Invest Ophthalmol Vis Sci, 2004. **45**(12): p. 4611-6.

45. Prusky, G.T., P.W. West, and R.M. Douglas, *Behavioral assessment of visual acuity in mice and rats.* Vision Res, 2000. **40**(16): p. 2201-9.

46. Payne, H.L. and J.L. Raymond, *Magnetic eye tracking in mice.* Elife, 2017. **6**.

47. Deneve, S., A. Alemi, and R. Bourdoukan, *The Brain as an Efficient and Robust Adaptive Learner.* Neuron, 2017. **94**(5): p. 969-977.

48. Paz, J.T. and J.R. Huguenard, *Microcircuits and their interactions in epilepsy: is the focus out of focus?* Nat Neurosci, 2015. **18**(3): p. 351-9.

49. Wiegert, J.S., et al., *Silencing Neurons: Tools, Applications, and Experimental Constraints.* Neuron, 2017. **95**(3): p. 504-529.

50. Wood, K.C., J.M. Blackwell, and M.N. Geffen, *Cortical inhibitory interneurons control sensory processing.* Curr Opin Neurobiol, 2017. **46**: p. 200-207.

51. Zheng, N. and I.M. Raman, *Synaptic inhibition, excitation, and plasticity in neurons of the cerebellar nuclei.* Cerebellum, 2010. **9**(1): p. 56-66.

52. Lepeta, K., et al., *Synaptopathies: synaptic dysfunction in neurological disorders - A review from students to students.* J Neurochem, 2016. **138**(6): p. 785-805.

53. Dostrovsky, J.O., J. Millar, and P.D. Wall, *The immediate shift of afferent drive to dorsal column nucleus cells following deafferentation: a comparison of acute and chronic deafferentation in gracile nucleus and spinal cord.* Exp Neurol, 1976. **52**(3): p. 480-95.

54. Jacobs, K.M. and J.P. Donoghue, *Reshaping the cortical motor map by unmasking*

latent intracortical connections. Science, 1991. **251**(4996): p. 944-7.

55. Dancause, N. and R.J. Nudo, *Shaping plasticity to enhance recovery after injury.* Prog Brain Res, 2011. **192**: p. 273-95.

56. Rajan, R., *Plasticity of excitation and inhibition in the receptive field of primary auditory cortical neurons after limited receptor organ damage.* Cereb Cortex, 2001. **11**(2): p. 171-82.

57. Tau, G.Z. and B.S. Peterson, *Normal development of brain circuits.* Neuropsychopharmacology, 2010. **35**(1): p. 147-68.

58. Tengolics, A.J., et al., *Response Latency Tuning by Retinal Circuits Modulates Signal Efficiency.* Sci Rep, 2019. **9**(1): p. 15110.

59. Geffen, M.N., S.E. de Vries, and M. Meister, *Retinal ganglion cells can rapidly change polarity from Off to On.* PLoS Biol, 2007. **5**(3): p. e65.

60. Wassle, H., et al., *Cone contacts, mosaics, and territories of bipolar cells in the mouse retina.* J Neurosci, 2009. **29**(1): p. 106-17.

61. Jones, B.W., et al., *Retinal remodeling in human retinitis pigmentosa.* Exp Eye Res, 2016. **150**: p. 149-65.

62. *AIDS tops cancer and blindness as 'most feared disease' in Gallup Survey.* Arch Ophthalmol, 1988. **106**(11): p. 1518.

63. Koch, S.F., et al., *Halting progressive neurodegeneration in advanced retinitis pigmentosa.* J Clin Invest, 2015. **125**(9): p. 3704-13.

Figure Legends:

Figure 1: Photoreceptor morphology in wild type mouse and rd10 mouse retinas.
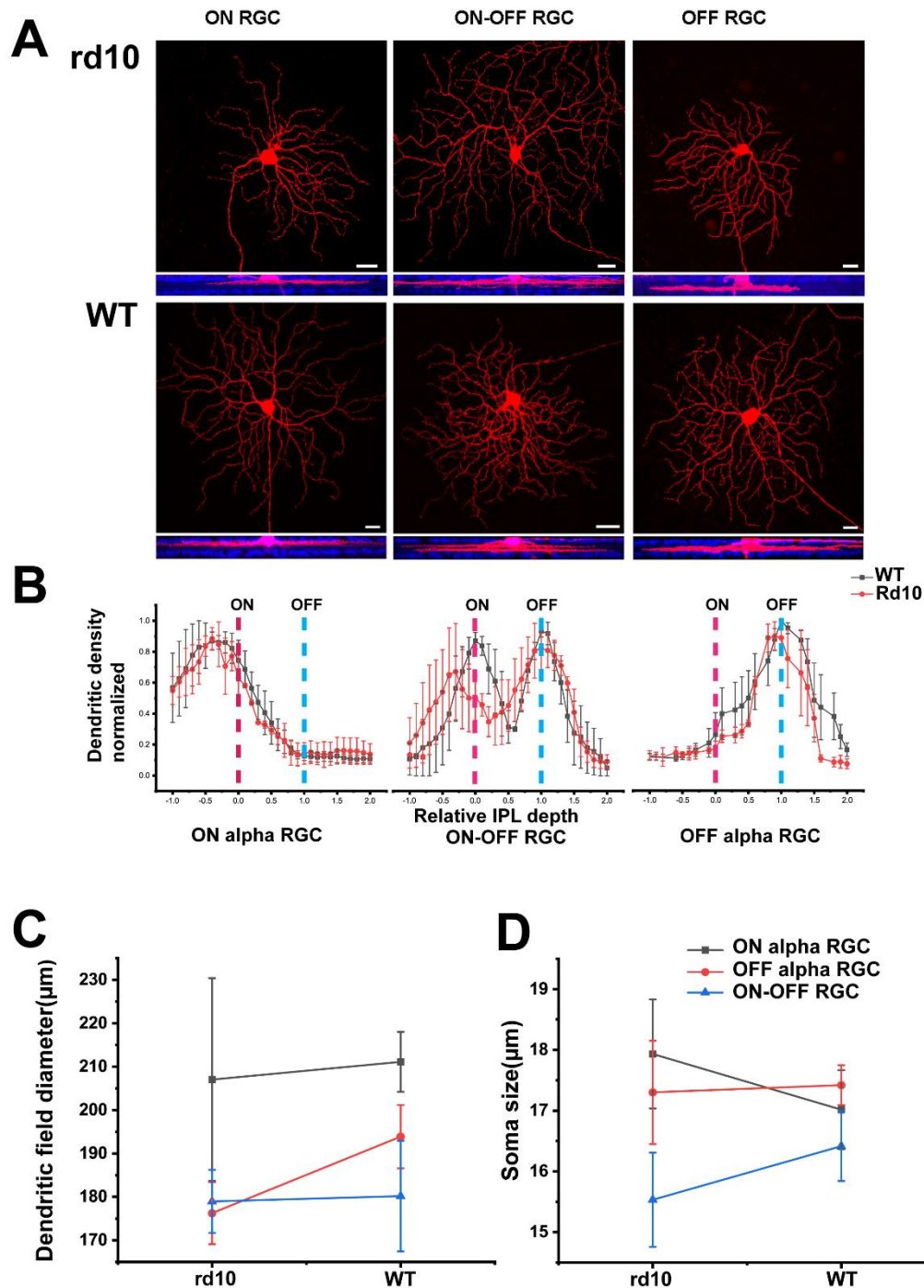
A: DAPI-Staining of vertical section of Wild Type (WT) P46 mouse retina. There are 12-15 layer of soma of photoreceptors in the outer nuclear layer (ONL)

B: Only 1-2 layer of soma of photoreceptors observed in P46 rd10 mouse retina.

C: The morphology of cone outer segments/inner segments labelled by red/green opsin of P46 wild type mouse retina appears normal.

D: The morphology of cone outer segments/inner segments in P46 rd10 mouse retina was disrupted. Opsin labelling shows cones lost their morphology and indicates have cells died.

Scale bar=20 μm

Figure 2: alpha ganglion cell in P46 rd10 and wild type mouse retinas.

A: ON, OFF alpha RGC, and ON-OFF RGC of P46 rd10 mouse retina show no obvious morphological damage compared to same types RGCs in WT mouse retinas with Neurobiotin injection. Lower images show cells double labelled with anti-ChAT antibody (blue).

Scale bar = 20 µm.

B: Stratification of ON, OFF alpha RGC, and ON-OFF RGCs in Rd10 and WT mouse. IPL depth is in normalized with 0 and 1 correspond to the ON and OFF ChAT bands, respectively (dashed lines). Bar mean density ± SEM (n = 3 cells).

C and D: Dendritic field equivalent diameter and somata size of ON, OFF alpha RGC, and ON-OFF RGC had no statistic difference between rd10 mice retinas and WT mice retinas.
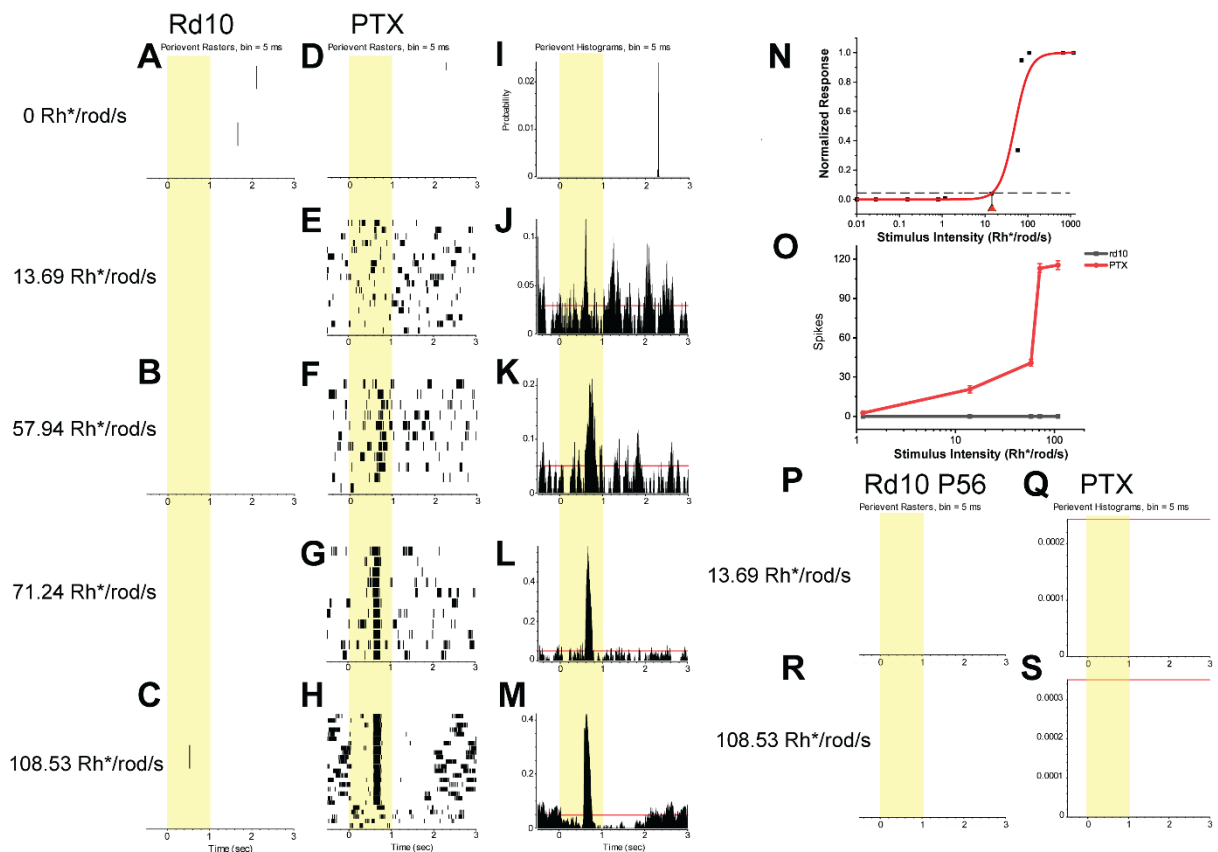
Figure 3: RGCs have similar cell responses in P46 rd10 and WT mouse retina.

Voltage –clamped of ON, OFF alpha RGC and ON-OFF RGCs from P46 rd 10 mouse retina at holding voltage of −68 mV (blue) and 0 mV (red) to isolate excitatory and inhibitory currents.

A: ON alpha RGC of both rd10 and WT mouse had light response to light stimulus1 second 525nm light stimuli (light intensity= 108.53 Rh*/rod/sec). Application 100µM PTX, decreased Inhibitory (red) currents but increased excitatory currents evoked by light. **B:** Application PTX also decreased Inhibitory (red) currents but increased excitatory currents evoked by light on OFF alpha RGC of both rd10 and WT mouse. **C:** Application PTX can decrease inhibitory currents of ON and OFF response, increase excitatory current of OFF response but no On response in WT retina. PTX only decrease inhibitory current of ON response in rd 10 retina. Asterisk indicated a statistically significant difference (P < 0.05)

D: Normalized changed of Inhibitory currents and excitatory currents after PTX application between rd10 and WT. RGCs have similar cell responses in P46 rd10 and WT mouse retina.

Figure 4: PTX application induced light response of ganglion cells in P46 rd10 mouse retina.

A-C: There was no light response of alpha like ganglion cells in P46 rd10 mouse retina with increased light stimulation (525 nm full field light stimulus from 0 to 108.53 Rh*/rod/s, light stimulation time: 1s).

D-H: raster plots of an alpha like RGC to same full-field light stimulus of increasing intensity after application of picrotoxin (PTX). Picrotoxin increased the threshold sensitivity of this RGC cell to approximately 34 Rh*/rod/s.
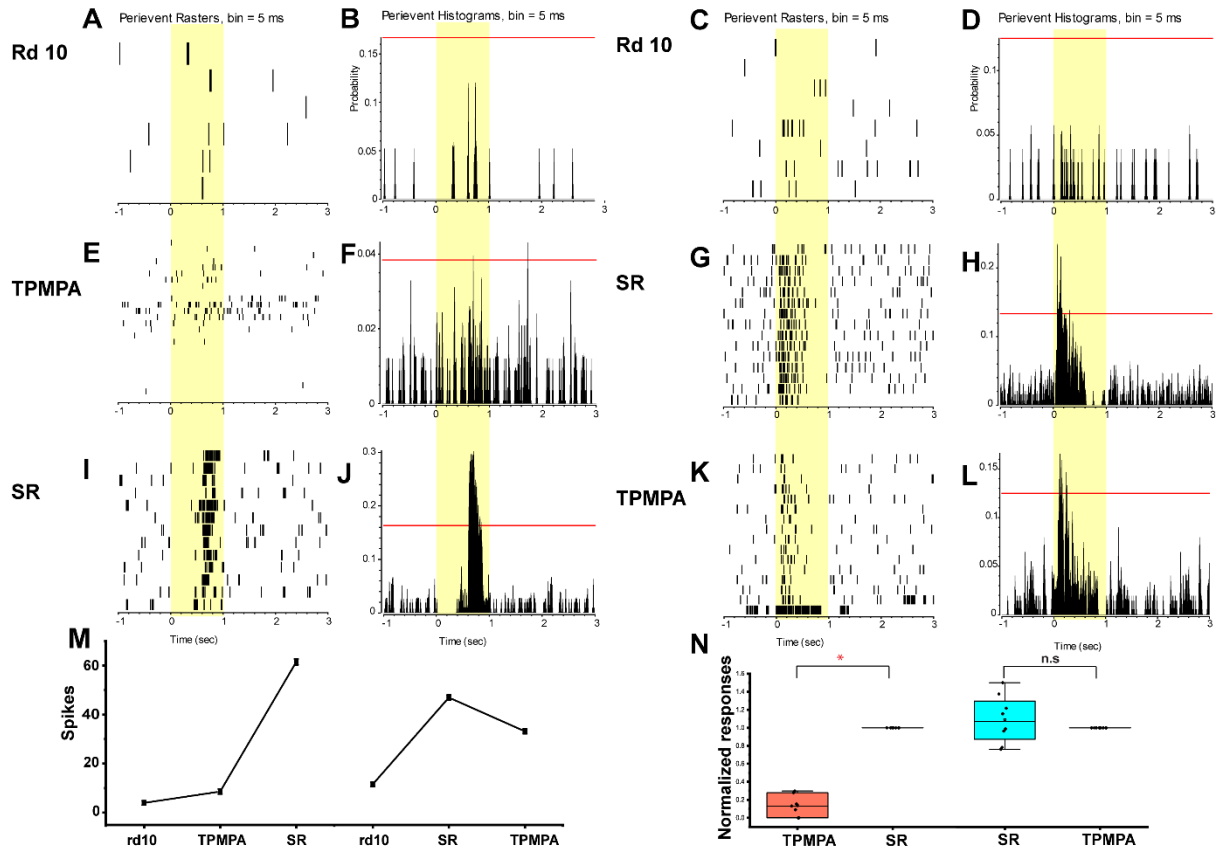
I-M: peristimulus time histogram of the alpha like RGC to increasing light intensity stimulus.

Picrotoxin increased the threshold sensitivity of this RGC cell to approximately 33 Rh*/rod/s.

N: Intensity–response plot of the RGC with data points fitted by a Michaelis–Menten equation. The threshold sensitivity of this RGC (16 Rh*/rod/s) was calculated as 5% of the maximal response (spike frequency) and is indicated by the arrowhead below (red triangle). **O**: Spikes increased after PTX application. Error bar in the figure indicates SEM within each group.

P, Q and R, S: As control, there was no light response of alpha RGC in P56 rd10 mouse retina and after PTX application. (525 nm full field light stimulus test at 13.69 and 108.53 Rh*/rod/s, light stimulation time: 1s).
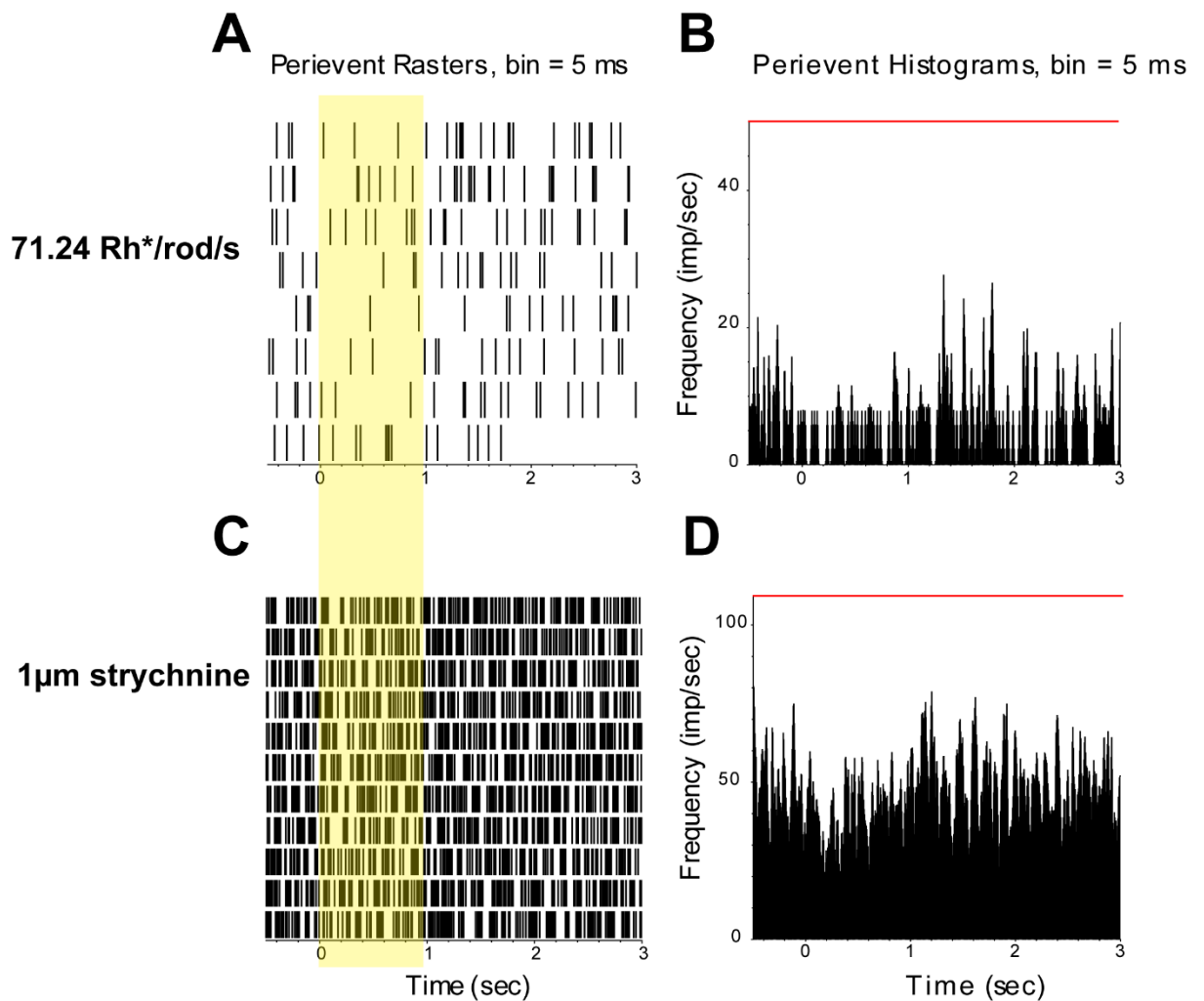
Figure 5: Effects of selective GABA receptor blockers on RGC in P43 rd10 mouse retina.

Effects of the GABA A-selective blocker gabazine (SR-95531, 10 μm) and the GABAC-selective blocker 1,2,5,6-tetrahydropyridin-4-yl-methylphosphinic acid (TPMPA, 100 μm) were determined in different sequence on the RGC in rd10 mouse retina. SR not TPMPA had a significant effect to restore the light response in rd10 mouse retina.

A, **C** (raster plots) and **B, D** (peristimulus time histogram) data show that RGC had no light response to 71.24 Rh*/rod/s in the rd10 mouse retina. **E** and **D** showed TPMPA application alone had no effect on the cell's light response, but subsequent application of SR induced the light response (**I** and **J**). Application SR alone induced a light response of RGC (**G** and **H**). Later TPMPA application did not change the light response.

M: Summary of spikes change from experiments A to L. Spikes mainly increased after SR application.

N: Normalized responses after sequencing application SR and TPMPA. Application SR had significant effect to induce the light response in rd10 mouse retina. The data are presented as averages. Error bars are SEM. Significance is based on student's t-test, where * $P < 0.05$, not statistically (n.s.). Significant $P > 0.05$.
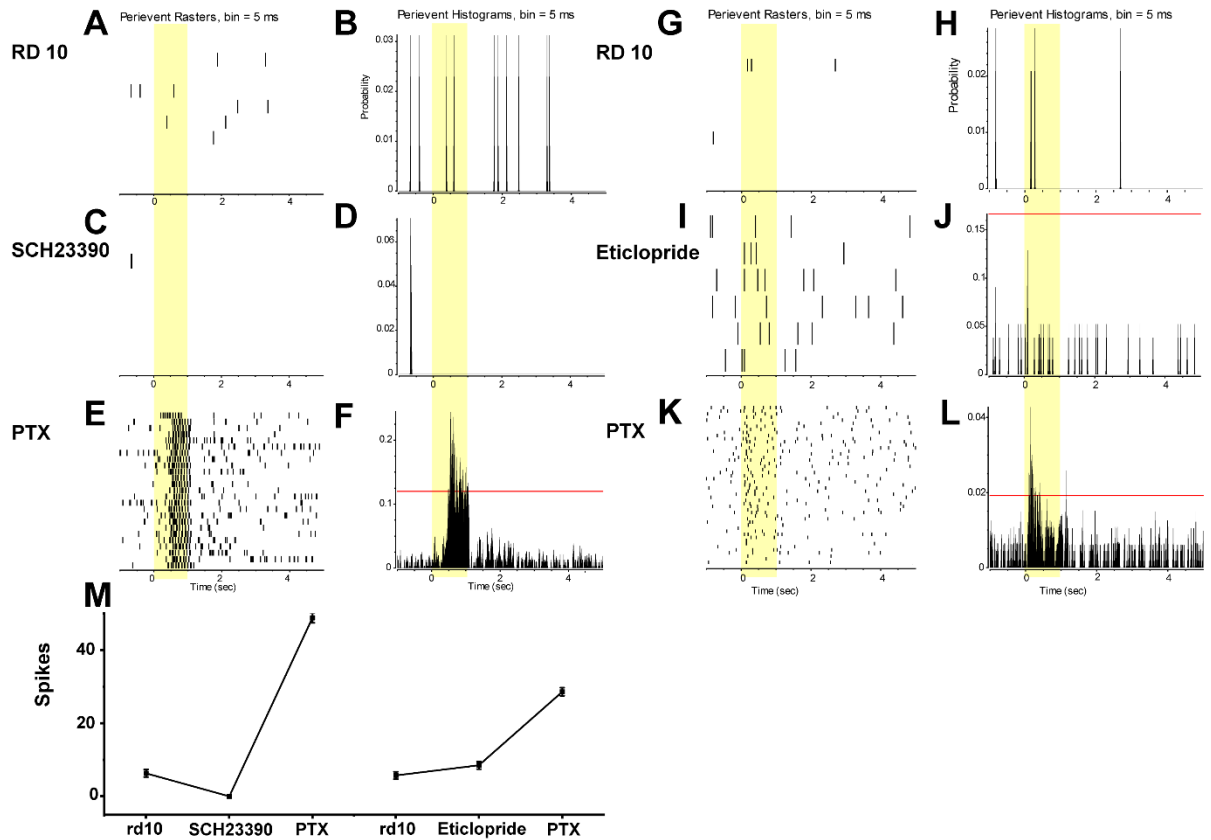
Figure 6: Effects of blocking selective glycine receptor on RGC light response in rd10 mouse retina.

A (raster plots) and **B** (peristimulus time histogram) data showing that RGC had no light response to 71.24 Rh*/rod/s in rd10 mouse retina. Application of the glycine receptor antagonist strychnine (1µM) did not induce a light response (**C** and **D**).
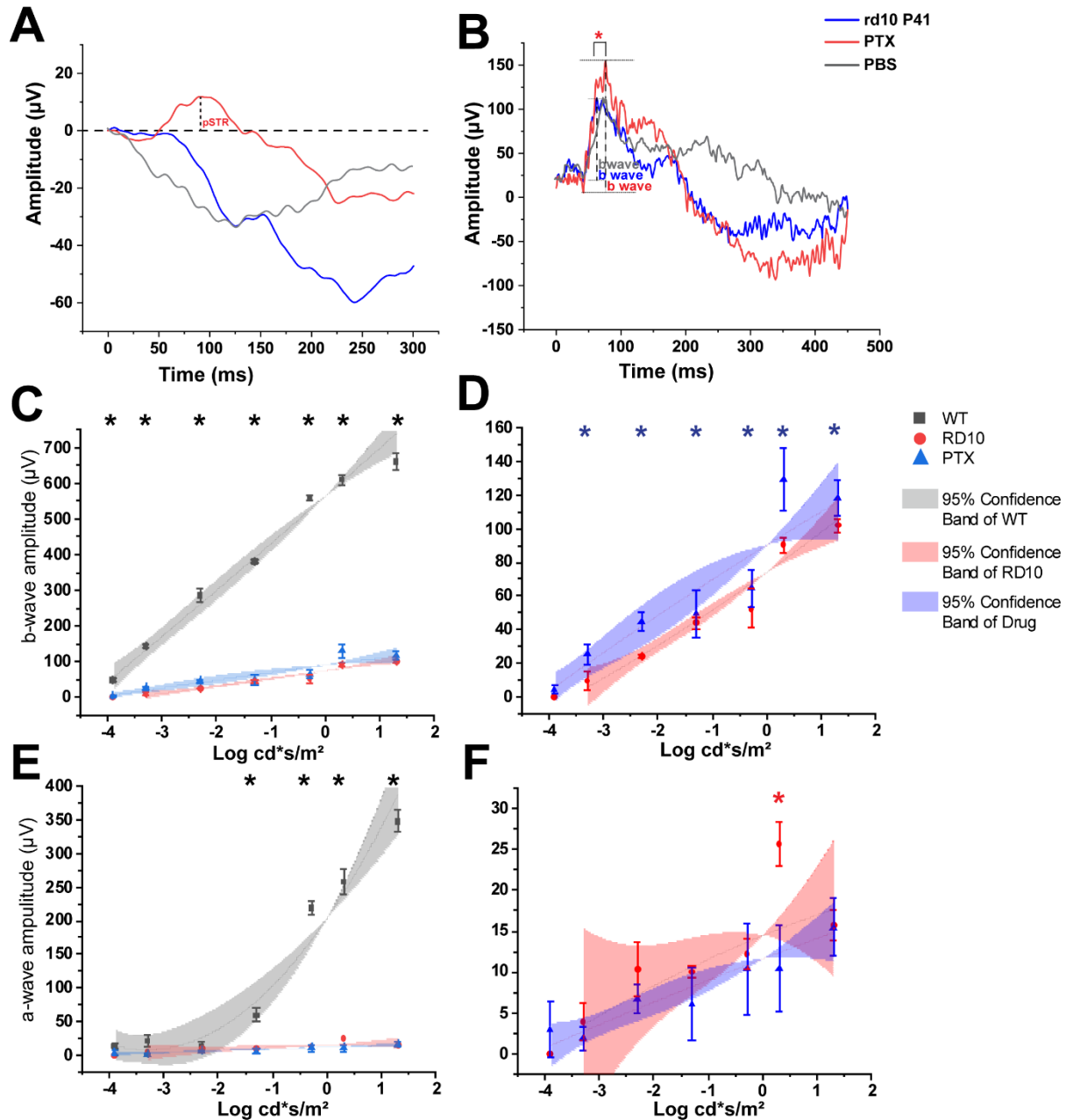
Red line is 95% confidence line.

Figure 7: Effects of blocking dopaminergic circuitry on RGC light response in rd10 mouse retina.

A, G (raster plots) and **B, H** (peristimulus time histogram) data showing that RGC had no light response to 71.24 Rh*/rod/s in rd10 mouse retina. Application of dopamine receptor 1 antagonist SCH 23390 (5 μM) or dopamine receptor 2 antagonist eticlopride (25 μM) alone did not induce light response of RGC (**C, D and I, J**). However, addition of 100 μM PTX induced a robust light response of the RGC in the rd10 mouse retina (**E, F and K, L**).

M: Spikes increased only after PTX application. Error bar in the figure indicates SEM within each group.
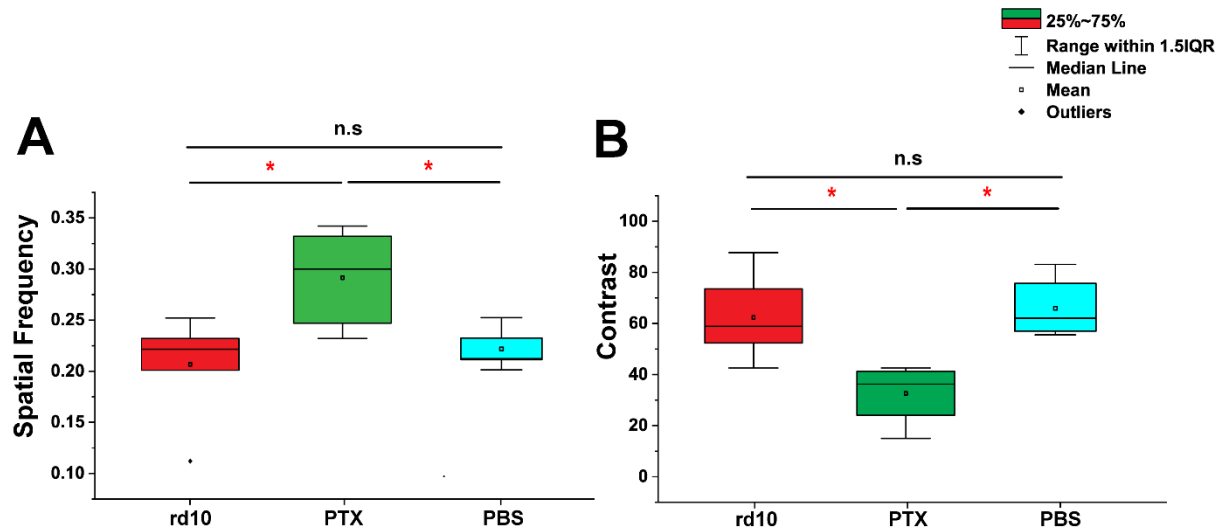
Figure 8: PTX induced STR and increased the amplitude of ERG b-wave but not a wave amplitude in P41 rd10 mouse retina.

The ERG response was noisy in P41 rd10 mouse retina, and no positive or negative scotopic threshold response (pSTR/nSTR) could be observed. After 0.015 mg/kg/d PTX application, pSTR appeared around 100ms (**A**). PBS application as vehicle control. Figure **B** showed wave traces recorded from P41 rd10 mouse and PTX application. PBS was applied as control.

Compared with wild-type mice, rd10 mice had significantly lower b-wave amplitudes in the scotopic range (P< 0.05) (**C and D**, **D** is enlarged image of **C**). Application of PTX significantly increased b-wave amplitudes (P<0.05) in rd10 mouse retina (**D**). However, PTX application did not increase amplitude of ERG a

wave at almost all intensities (P> 0.05, except 0.3 cd*s/m^2 , p<0.05) (**E and F**, **F** is enlarged image of **E**).

Polynomial fitting was applied from Figure C to F. Error bar in the figure indicates SEM within each group. Significance is based on student's t-test, where * P < 0.05.

Figure 9: Application of PTX leads to increase in behavioural measures of spatial vision in rd10 mouse eyes.

Photopic optomotor responses from P41 eyes of rd10 with PTX application significantly（$p<0.05$）increased both visual acuity (A, spatial frequency) tested at 100% contrast and contrast sensitivity (B, tested at 0.092 cycle/degree) and 1.5-Hz temporal frequency. PBS loaded as vehicle control had no statistic difference to the rd10 untreated group. For all panels, data are presented as mean ± SEM, Significance is based on unpaired student's t-test, where * $P < 0.05$.